



Transcriptome Analyses Reveal Candidate Pod Shattering-Associated Genes Involved in the Pod Ventral Sutures of Common Vetch (*Vicia sativa* L.)

Rui Dong¹, Deke Dong¹, Dong Luo¹, Qiang Zhou¹, Xutian Chai¹, Jiyu Zhang¹, Wengang Xie¹, Wenxian Liu¹, Yang Dong², Yanrong Wang^{1*} and Zhipeng Liu^{1*}

¹ State Key Laboratory of Grassland Agro-ecosystems, College of Pastoral Agriculture Science and Technology, Lanzhou University, Lanzhou, China, ² State Key Laboratory of Systematic and Evolutionary Botany, Institute of Botany, Chinese Academy of Sciences, Beijing, China

OPEN ACCESS

Edited by:

Maoteng Li,
Huazhong University of Science and
Technology, China

Reviewed by:

Sushma Naithani,
Oregon State University, USA
Liezhaio Liu,
Southwest University, China

*Correspondence:

Yanrong Wang
yrlwang@lzu.edu.cn
Zhipeng Liu
lzp@lzu.edu.cn

Specialty section:

This article was submitted to
Crop Science and Horticulture,
a section of the journal
Frontiers in Plant Science

Received: 29 December 2016

Accepted: 10 April 2017

Published: 27 April 2017

Citation:

Dong R, Dong D, Luo D, Zhou Q,
Chai X, Zhang J, Xie W, Liu W, Dong Y,
Wang Y and Liu Z (2017)
Transcriptome Analyses Reveal
Candidate Pod Shattering-Associated
Genes Involved in the Pod Ventral
Sutures of Common Vetch (*Vicia
sativa* L.). *Front. Plant Sci.* 8:649.
doi: 10.3389/fpls.2017.00649

The seed dispersion caused by pod shattering is a form of propagation used by many wild species. Loss of seeds from pod shattering is frequent in the common vetch (*Vicia sativa* L.), an important self-pollinating annual forage legume. However, pod shattering is one of the most important defects that limits the reproduction of the vetch in the field and the usage as a leguminous forage crop. To better understand the vetch pod shattering mechanism, we used high-throughput RNA sequencing to assess the global changes in the transcriptomes of the pod ventral sutures of shattering-susceptible and shattering-resistant vetch accessions screened from 541 vetch germplasms. A total of 1,285 significantly differentially expressed unigenes (DEGs) were detected, including 575 up-regulated unigenes and 710 down-regulated unigenes. Analyses of Gene Ontology and KEGG metabolic enrichment pathways of 1,285 DEGs indicated that 22 DEGs encoding cell wall modifications and hydrolases associated with pod shattering were highly expressed in shattering-susceptible accessions. These genes were mainly enriched in “hydrolase activity,” “cytoplasm,” and “carbohydrate metabolic process” systems. These cell wall modifications and hydrolases genes included β -glucosidase and endo-polygalacturonase, which work together to break down the glycosidic bonds of pectin and cellulose, and to promote the dissolution and disappearance of the cell wall in the ventral suture of the pod and make the pod more susceptible to shattering. We demonstrated the differences in gene transcription levels between the shattering-susceptible and shattering-resistant vetch accessions for the first time and our results provided valuable information for the identifying and characterizing of pod shattering regulation networks in vetch. This information may facilitate the future identification of pod shattering-related genes and their underlying molecular mechanisms in the common vetch.

Keywords: *Vicia sativa* L., transcriptome, pod ventral suture, pod shattering, cell wall hydrolases

INTRODUCTION

In nature, seed dispersal or fruit dehiscence is an essential process in the proliferation of wild plants (Funatsuki et al., 2014). This process can be used to ensure adequate growth space for the progeny of plants in nature (Funatsuki et al., 2014). This agronomic trait exists in most Leguminosae, Gramineae, and Brassicaceae crops, such as common vetch (*Vicia sativa* L.) (Abd El-Moneim, 1993), soybeans (*Glycine max* L.) (Christiansen et al., 2002), rice (*Oryza sativa* L.) (Dong et al., 2014), thale cress (*Arabidopsis thaliana* L.) (Dong et al., 2014) and oilseed rape (*Brassica napus* L.) (del Carmen Rodríguez-Gacio et al., 2004). However, since the domestication of plants began, humans have attempted to breed non-shattering crop varieties to reduce seed dispersal, because this agronomical trait leads to a reduction in seed yield (Funatsuki et al., 2006; Dong et al., 2014). Harvesting pod shattering-susceptible soybean varieties in dry weather conditions during the harvest period can lead to seed losses of 50–100% (Bhor et al., 2014). For oilseed rape, average annual seed losses due to pod shattering are ~20–50% of the total seed yield. Therefore, eliminating pod shattering would in theory produce an equivalent increase in harvested yield (Squires et al., 2003; Østergaard et al., 2006; Raman et al., 2014). In addition, seeds dispersed by pod shattering can persist in the soil seed bank for up to 10 years, thus leading to the appearance of a crop as a weed in subsequent crop growing seasons (Pekrun et al., 1997). Therefore, resistance to pod shattering has been preferentially selected for during domestication as the most important domestication trait (Funatsuki et al., 2014).

In plants, seed dispersal or pod shattering has been revealed to be associated primarily with the separation, elimination or modification of the dehiscence zone tissue cells (Dong et al., 2014). Adhesion between cells is a fundamental feature of plant growth and development and is an important factor in maintaining the mechanical strength of plants. In dicotyledonous plants, the adherent region is occupied by a network of various pectin polymers. When the plant cells separate, the pectin polymer network of the adherent cells decomposes in the local tissue. This phenomenon occurs during pod shattering, seed dispersal and fruit ripening (Jarvis et al., 2003). Enzymatic cleavage of the galacturonan chain of pectin is an effective method of solubilizing pectin, and usually separates dicotyledonous cells (Zhang et al., 2000; Jarvis et al., 2003). Polygalacturonases have been found to be involved in the hydrolysis of pectin in many stages of plant development, particularly in tissues that require cell separation (Hadfield and Bennett, 1998). Previous studies have shown that some specific genes are expressed during the plant abscission process. The products of these genes include polygalacturonase, $\beta(1,4)$ -D-glucanase and other enzymes (Hong and Tucker, 1998). In addition, most of these enzymes belong to the isotype specific to the abscission zone. The network of cellulose and hemicellulose is also a major component of the plant primary cell wall. In *Arabidopsis* and other dicotyledons, xyloglucan is the major cell wall hemicellulose (Lashbrook and Cai, 2008). Other cell wall modification enzymes also play an important role in the

breakdown of the cell wall and the degradation of the dehiscence zone, such as endo-polygalacturonase, pectin methylesterases and β -galactosidase (Christiansen et al., 2002; Tavarini et al., 2009; Zhang et al., 2012). One of the most notable enzymes is the endo-galacturonase *RDPG1*, which has been shown to promote the breakdown of the middle lamella (Christiansen et al., 2002). Several genes encoding transcription factors required for silique development and shattering in *Arabidopsis* have been extensively studied at the molecular level (Zhang et al., 2016).

In recent years, several soybean pod shattering studies have obtained exciting results. Researchers have found a key new cellular feature in the abscission layer of the shattering-resistant soybean pod ventral suture, called fiber cap cells (FCC) (Dong et al., 2014). Increased expression of the *GmSHAT1-5* gene leads to increased thickening of the secondary cell wall of FCC, thus preventing pod shattering in the domesticated soybean. Furthermore, removing repressive elements enhances the expression of *GmSHAT1-5* in the FCC and promotes the over-deposition of the secondary cell wall (Dong et al., 2014). Another functional gene, *pdh1*, has been found to be highly expressed in the lignin-rich internal sclerenchyma of soybean pod walls, particularly at the initial stage of lignin deposition (Funatsuki et al., 2014). A comparison of near isogenic lines has shown that *pdh1* promotes pod shattering by increasing the torsion force of the dry pod wall, which is a driving force of pod shattering in dry climates (Funatsuki et al., 2014).

The common vetch is an important self-pollinating annual forage legume (Chung et al., 2013; Liu et al., 2013a; Dong et al., 2016a). Owing to its broad environmental adaptation and high nutritional value, it is used for hay production, pasture, silage, and green manure (Sullivan and Diver, 2003; Liu et al., 2014; Kim et al., 2015; Dong et al., 2016a). It is widely planted in Turkey, Australia, New Zealand, the Qinghai-Tibetan plateau of China and other parts of the world (Dong et al., 2016a). In Turkey, the planted area of the common vetch has reached 579,684 ha (Firincioglu, 2012). However, the shattering of mature vetch pods is one of the most important defects limiting its utilization (Abd El-Moneim, 1993). The results of hybridization of shattering-susceptible and shattering-resistant accessions have indicated that the F2 populations are separated according to a 3:1 ratio (susceptible: resistant) (Abd El-Moneim, 1993). In addition, the research regarding vetch pod shattering is still at a preliminary level of phenotypic observation (van de Wouw et al., 2003). Next-generation sequencing (NGS) is currently the preferred method for understanding gene expression in non-model plants at different developmental stages on a transcriptome-wide scale (Liu et al., 2016). By comparing the transcriptomes of the pod ventral sutures of shattering-susceptible and shattering-resistant accessions screened from 541 vetch accessions, the present study provides a good understanding of the genetic basis of pod shattering in the common vetch, which exhibits different dehiscence zone structures from those of *Arabidopsis* and soybeans. This study provides additional genetic information for the study of plant pod shattering.

MATERIALS AND METHODS

Plant Materials and Sample Collection

A total of four common vetch accessions were used in this study: 92, 135, 257, and 392. The four accessions were screened from 541 vetch accessions by evaluation of the pod shattering index in three consecutive years (2012–2014). Seeds of these four vetch accessions were provided by the National Plant Germplasm System of the United States and Lanzhou University, China. The seeds were sown in the Yuzhong Experimental Station of Lanzhou University (N 35°57', E 104°09', 1,720 m above sea level), Lanzhou, China. The mean annual precipitation in this area is 350 mm, and the mean annual temperature is 6.7°C.

At flowering time, 400 flowers were tagged for each accession on different plants. The pod ventral sutures of the four accessions were the samples used in this study (Figure 1). Pod ventral sutures were selected as the material for the study of pod shattering because our previous study has found that vetch pod shattering is initiated in the pod ventral suture.

The sampling time was the period of time required for the formation of the dehiscence zone in the pod ventral sutures. Because the growth periods of the different vetch accessions were not consistent, the collection time of the samples from the four accessions was different. The detailed collection times are shown in Table S1. At the time of sampling, the seed size was approximately one-third of the final size, and the pod length and width were 80–90% those of the mature yellow pod. The pods were collected and placed on ice, and the pod ventral sutures were manually removed. The freshly removed pod ventral suture samples were immediately frozen in liquid nitrogen and stored at –80°C for RNA isolation.

Pod Shattering Index Evaluation

The pod shattering rate and pod shattering mechanical force were used to evaluate the pod shattering index of the four accessions. Under field conditions (without artificial disturbance), the number of shattering pods of each accession was counted out of 100 pods after pod maturity in three consecutive years (2012–2014). Under laboratory conditions, 100 mature pods were collected for each accession, air-dried at room temperature for 2 weeks, and kept in an oven at 37°C for 24 h, and the minimum mechanical force necessary to break the pods from

the different accessions into two parts was measured by using a digital mechanical force gauge (HANDPI, China) (Dong et al., 2014, 2016b). All statistical analyses were performed on three replicates.

Polygalacturonase and Cellulase Activity Assays

The activity of polygalacturonase and cellulase (β -1,3;1,4-glucanase) in the pod ventral sutures of the four accessions was determined. Polygalacturonase activity was determined using the method described by Lohani et al. (2004) and Gross (1982). Cellulase (β -1,3;1,4-glucanase) activity was measured according to the reducing groups released from carboxymethyl cellulose (CMC), as described by Wu et al. (2008).

Pod Ventral Suture Structure

The pod ventral suture structures from the four different accessions were frozen during the sampling period, and frozen sections were then observed. The pod samples were fixed with FAA fixation solution for 24 h and embedded in OCT (Sakura, USA) embedding agent, and 5 μ m sections were then dissected using a cryostat (LEICA CM3050S, Germany) and analyzed using an OLYMPUS microscope (OLYMPUS BX51, Japan) (Kawamoto, 2003).

RNA Extraction and Library Construction for Transcriptome Analysis

Total RNA of the four accessions was extracted using Trizol reagent according to the manufacturer's instructions (Invitrogen, Carlsbad, CA, USA). The RNA concentrations were determined using a Qubit[®] RNA Assay Kit and a Qubit[®] 2.0 Fluorometer (Life Technologies, CA, USA), and the RNA integrity was assessed using an RNA Nano 6000 Assay Kit with an Agilent Bioanalyzer 2100 system (Agilent Technologies, CA, USA). Poly(A)-containing mRNAs were purified from the total RNA with oligo (dT) magnetic beads (Illumina, San Diego, CA). Then, mRNA random fragmentation, cDNA synthesis, purification and PCR amplification were performed according to the Illumina RNA-Seq protocol. The four cDNA libraries were sequenced with a read length of 194 bp on a HiSeq 2000 system with a paired-end module at Biomarker Co. Ltd. (Beijing, China).

Sequence Filtering, *De novo* Assembly and Functional Annotation

The raw sequencing reads were cleaned by using the FASTX toolkit. A *de novo* transcriptome assembly of all the reads was performed using the Trinity Program (Grabherr et al., 2011). According to the Trinity assembly results, all unigenes were annotated on the basis of a BLASTx alignment, with 10^{-5} as the *E*-value cut off point, to sequence comparisons with public databases, including the NCBI non-redundant protein sequences (Nr), Gene Ontology (GO), Clusters of Orthologous Groups of proteins (COGs), Kyoto Encyclopedia of Genes and Genomes (KEGG), and Swiss-Prot protein databases. The amino acid sequences of the unigenes were predicted and compared against the Pfam protein database using HMMER 3.0 (E -value $\leq 1e^{-10}$) to obtain unigene domain/family annotation information. The

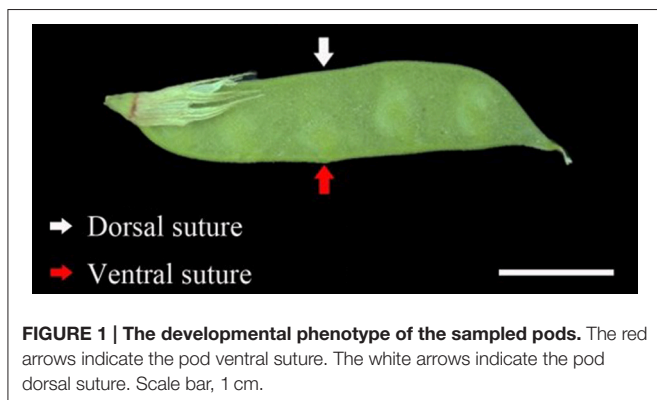


FIGURE 1 | The developmental phenotype of the sampled pods. The red arrows indicate the pod ventral suture. The white arrows indicate the pod dorsal suture. Scale bar, 1 cm.

results that aligned best against the five protein databases were used to determine the sequence directions of the unigenes. The BLAST hits were analyzed using Blast2GO software to obtain GO terms to retrieve molecular function, biological process and cellular component descriptions (Liu et al., 2013b; Calzadilla et al., 2016). The GO annotation functional classifications were determined using WEGO software for the distribution of gene functions (Ye et al., 2006).

Differential Expression Analysis

The reads obtained from the sequencing of each sample were compared against the unigene library by using Bowtie, and the expression was calculated according to the alignment results and RSEM (Langmead et al., 2009; Li and Dewey, 2011; Langmead and Salzberg, 2012). The differential expression analysis was performed using the MARS method in the DEGseq 2010 R package (Anders and Huber, 2010; Wang et al., 2010). The analysis was performed using Benjamini and Hochberg correction of the *p*-values and finally using the corrected *p*-value and the FDR (False Discovery Rate) to reduce false positives (Benjamini and Hochberg, 1995; Sivankalyani et al., 2016). The *p*-value was adjusted using the *q*-value (Shannon et al., 2003). A *q*-value < 0.005 and an absolute value of the log₂ (fold change) > 1 were used as thresholds for determining the significant DEGs. The DEG expression patterns were clustered using STEM software (*p*-value ≤ 0.05). A GO enrichment analysis was performed for all the DEGs using topGO software and agriGO, and KOBAS 2.0 was used to carry out the KEGG pathway enrichment analysis (Liu et al., 2016).

Quantitative Real-Time PCR Analysis

A portion of the total RNA of the four samples used for the RNA-Seq analysis was used to make cDNA for qRT-PCR analysis. An M-MuLV First Strand cDNA Synthesis Kit (TaKaRa Biotechnology, Dalian, China) was used according to the manufacturer's instructions to generate cDNA from 1 μg of total RNA from each sample. The cDNA samples were diluted to a concentration of 1 ng/ml. Quantitative qRT-PCR was performed using an iQ 5 Multicolor Real-time PCR Detection system (Bio-Rad, USA) and Power SYBR Green Master Mix (Applied Biosystems), by following the manufacturer's protocol (TaKaRa SYBR Premix Ex Taq II Kit, Dalian, China). Unigene 68614, with unknown function, was selected as an internal control gene, owing to its relatively stable expression in the common vetch transcription profiles (Liu et al., 2013a). Specific primers for qRT-PCR were designed by using Primer Express software and are shown in Table S2. The qRT-PCR analysis of each sample was performed in triplicate. The expression levels of each unigene were normalized to that of unigene 68614, and the relative gene expression levels were calculated using the $2^{-\Delta\Delta Ct}$ method.

RESULTS

Pod Shattering Index

In this study, the pod shattering rate and pod shattering mechanical force of accessions Nos. 92, 257, 135, and 392

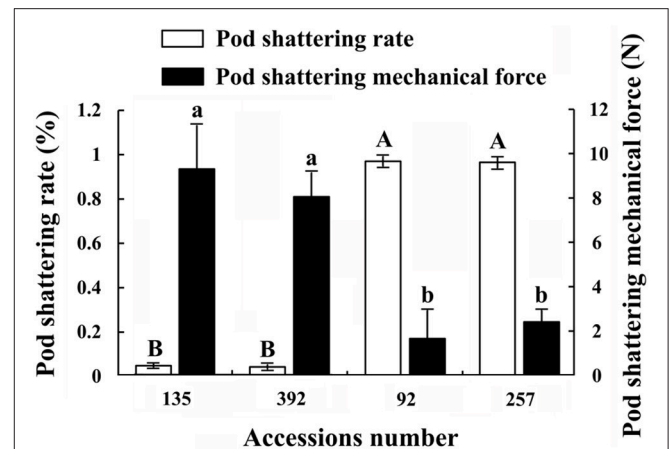


FIGURE 2 | Pod shattering rate and pod shattering mechanical force of four common vetch accessions. Pod shattering rate refers to the rate of pod shattering in the field (without artificial disturbance). Three replicates, each with 100 pods, were observed. Values represent mean ± SE. Pod shattering mechanical force refers to the minimum mechanical force necessary to break the pods of different accessions into two parts. This experiment was repeated three times, with 100 pods measured each time. Values represent mean ± SE. Different uppercase and lowercase letters indicate significant differences among the different accessions at *p* < 0.01 according to Tukey's test.

showed significant differences (Figure 2). The results of the pod shattering rate analysis confirmed that Nos. 92 and 257 were pod shattering-susceptible accessions, with pod shattering rates higher than 95%, whereas Nos. 135 and 392 were pod shattering-resistant accessions, with pod shattering rates lower than 5% (Figure 2). Furthermore, the average pod shattering mechanical force of Nos. 135 and 392 was approximately four times that of Nos. 92 and 257 (Figure 2). Figure 3 shows more details of pod shattering in the shattering-susceptible and shattering-resistant accessions under field and low humidity conditions.

Polygalacturonase and Cellulase Activity of Pod Ventral Sutures

Polygalacturonase and cellulase (β-1,3;1,4-glucanase) are important hydrolases in the cell wall. The results showed that the activities of polygalacturonase and cellulase (β-1,3;1,4-glucanase) were significantly higher in the pod ventral sutures of the shattering-susceptible accessions than in those of the shattering-resistant accessions (Figures 4, 5). The polygalacturonase activity was highest in accession 257 and lowest in accession 135. The cellulase activity was highest in accession 92 and lowest in accession 135.

Pod Ventral Suture Structure

Figure 6 shows the structure of pod ventral suture samples that were manually removed. Cross sections of pod ventral sutures of the shattering-susceptible and shattering-resistant accessions showed that both had vascular bundle structures in the pod ventral sutures (Figure 6). In the pod shattering-susceptible accessions, the vascular bundles were separated into two sections



by a dehiscence zone (Figure 6B), whereas the pod shattering-resistant accessions did not have a dehiscence zone, and the vascular bundles in these pods were not separated (Figure 6A).

Transcriptome Sequencing and *De novo* Assembly

RNA samples from the pod ventral sutures of the four accessions were used to construct cDNA libraries. A total of 145,891,066 raw reads were ultimately obtained from the four libraries. After a stringent quality check and data filtering, a total of 104,234,410 reads and 26.2 GBase of data were obtained (Table 1). The Q20 values of all four samples were higher than 98.5%. Figure S1 shows the sequencing results in more detail. A total of 496,337

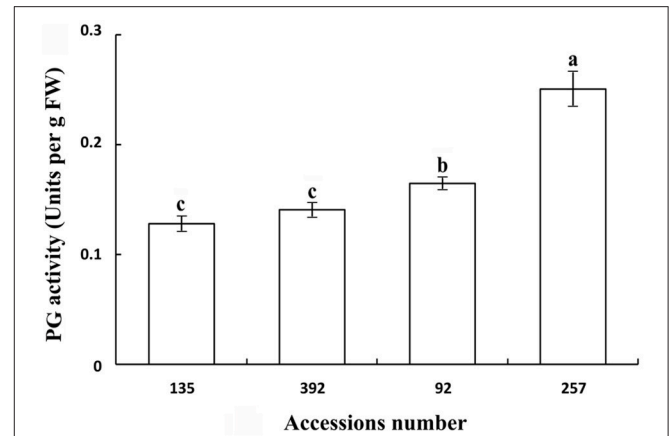


FIGURE 4 | Polygalacturonase activity in pod ventral sutures of four common vetch accessions. One unit of polygalacturonase activity is the amount that catalyses the formation of 1 μ m of reducing groups per min per g of original fresh weight of pod ventral sutures of the common vetch. PG refers to polygalacturonase. Three replicates were performed, each replicate measuring 30 pod ventral sutures. For each replicate, 30 pods of the ventral sutures were collected, and the 30 pod ventral suture samples were mixed for measurement. Values represent mean \pm SE. Different lowercase letters indicate significant differences among the different accessions at $p < 0.01$ according to Tukey's test.

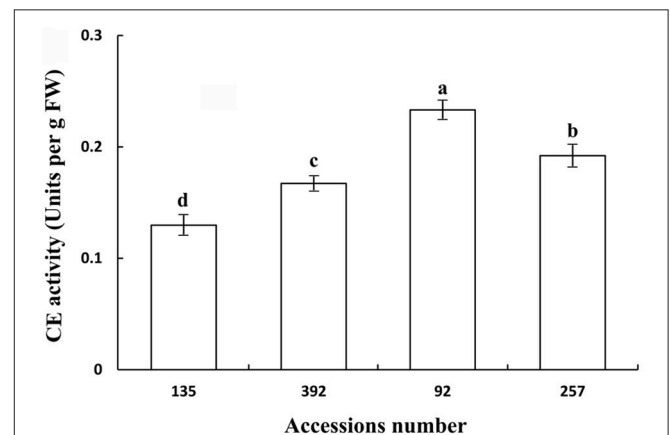


FIGURE 5 | Cellulase (β -1,3;1,4-glucanase) activity in pod ventral sutures of four common vetch accessions. One unit of cellulase activity is defined as the amount of the enzyme required to release 1 μ m of reducing groups per min per g of original fresh weight of pod ventral sutures of the common vetch. CE refers to cellulase. Three replicates were performed, each replicate measuring 30 pod ventral sutures. For each replicate, 30 pods of the ventral sutures were collected, and the 30 pod ventral suture samples were mixed for measurement. Values represent mean \pm SE. Different lowercase letters indicate significant differences among the different accessions at $p < 0.01$ according to Tukey's test.

contigs (≥ 100 bp) were obtained, wherein the N50 of the contigs was 126 bp, and the average size of the contigs was 71 bp. Figure S2 shows the distribution of the contig assembly. The total contigs were assembled into 70,742 unigenes, and 47,921 unigenes were identified for No. 92, 44,922 for No. 135, 45,325

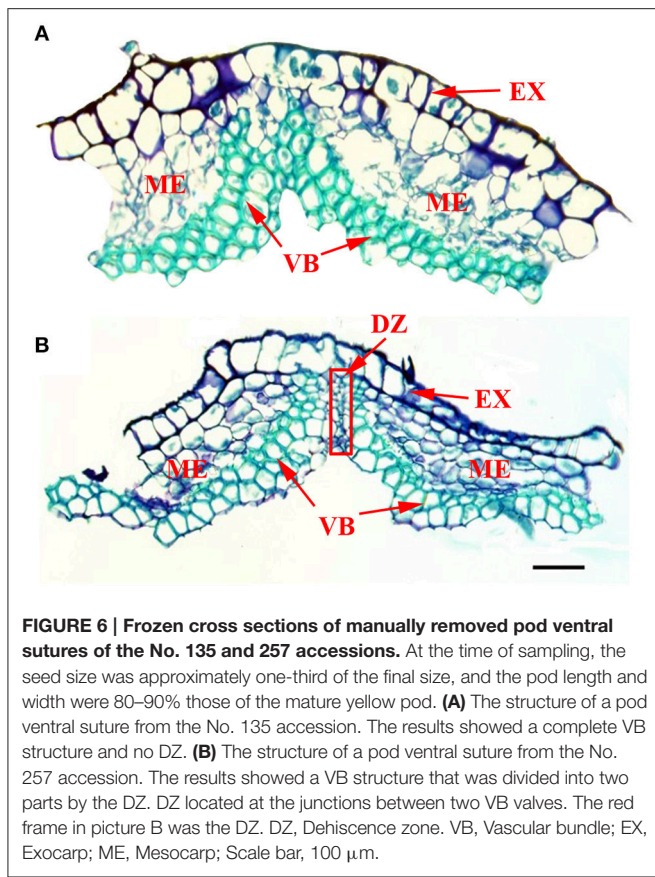


FIGURE 6 | Frozen cross sections of manually removed pod ventral sutures of the No. 135 and 257 accessions. At the time of sampling, the seed size was approximately one-third of the final size, and the pod length and width were 80–90% those of the mature yellow pod. **(A)** The structure of a pod ventral suture from the No. 135 accession. The results showed a complete VB structure and no DZ. **(B)** The structure of a pod ventral suture from the No. 257 accession. The results showed a VB structure that was divided into two parts by the DZ. DZ located at the junctions between two VB valves. The red frame in picture B was the DZ. DZ, Dehiscence zone. VB, Vascular bundle; EX, Exocarp; ME, Mesocarp; Scale bar, 100 μm .

TABLE 1 | Summary of the transcriptome data.

Sample	Total raw reads	Total clean reads	Total clean nucleotides (nt)	Q20 (%)	Unigenes
135	43,293,509	27,925,411	7.0 G	98.64	44,922
392	41,401,651	26,212,623	6.6 G	98.63	43,603
92	31,179,196	24,103,592	6.1 G	98.56	47,921
257	30,016,710	25,992,784	6.5 G	98.65	45,325
Total	145,891,066	104,234,410	26.2 G		70,742

for No. 257 and 43,603 for No. 392 (Table 1). The N50 of these unigenes was 1,309, and the mean length was 772 bp. Of the 70,742 unigenes, 39,339 unigenes (55.61%) were between 200 and 500 bp, 14,539 unigenes (20.55%) were between 501 and 1,000 bp, and 16,861 unigenes (23.84%) were longer than 1,000 bp (Figure S3). The reads of this study have been deposited in the NCBI SRA database (SRX2400610).

Functional Annotation and Classification

The results indicated that 42,074 (59.48%) unigenes were annotated and aligned to known proteins in the Nr database and that 26,134 (36.94%) were aligned to sequences in the Swiss-Prot database (Table S3). In addition, 3,691 (5.22%) unigenes were annotated in all seven databases, and 46,763 (66.10%) unigenes

were annotated in at least one database (Table S3). Further analysis of the matching sequences revealed that 32.82% of the sequences had the closest match to sequences from *Medicago truncatula* (Figure S4).

GO assignments were used to classify the functions of the predicted pod ventral suture genes in vetch. In this study, 23,533 unigenes were assigned to a total of 51 GO functional groups and 22,383 GO annotations, which fell into the three main categories (Figure S5). A total of 37,193 unigenes were distributed under the cellular component category, 28,411 unigenes were distributed under the molecular function category, and 59,076 unigenes were distributed under the biological process category.

All the unigenes were assigned to COGs for further functional prediction and classification. In total, 17,281 unigenes were assigned to 25 COG classifications (Figure S6). Among the 25 COG categories, the class “general function prediction only” (16.69%) represented the largest group and was followed by “replication, recombination and repair” (8.57%) and “transcription” (8.05%).

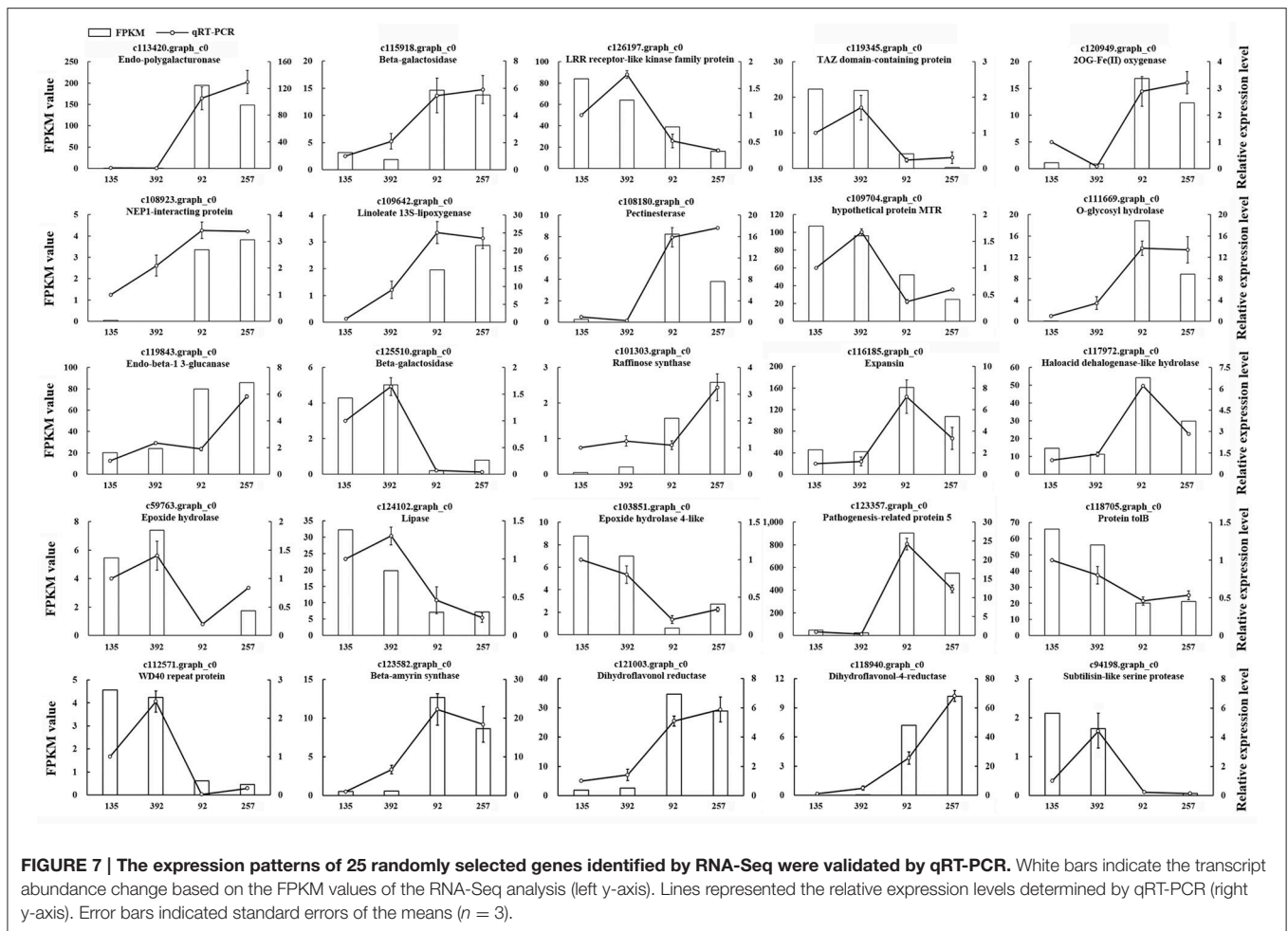
To explore the pathways that involved these annotated genes, the unigenes were also compared against the KEGG database. As a result, a total of 15,571 annotated unigenes had significant matches with 16,070 hits in the KEGG database and were assigned to 127 KEGG pathways (Table S4). Of these unigenes, 10,453 were assigned to the metabolic pathway, which is the largest group of the five categories classified by KEGG (Figure S7A). The 10,453 metabolic pathway genes were further classified into 18 subcategories (Figure S7B), most of which mapped to carbohydrate metabolism (2,486), translation (1,663) and amino acid metabolism (1,622).

qRT-PCR Verification

To verify the accuracy and reproducibility of the RNA-seq analysis, 25 unigenes were randomly selected for quantitative real-time PCR (qRT-PCR) validation (Table S2). The expression profiles of these 25 unigenes determined by qRT-PCR were consistent with the RNA-seq data (Figure 7). A linear regression analysis showed a significant positive correlation (Pearson correlation coefficient, $r = 0.87$) between the gene expression ratios determined by the two different methods, thus indicating that our RNA-seq data were reliable.

Analysis of Differentially Expressed Genes (DEGs)

Based on strict criteria, there were 1,285 unigenes that were differentially expressed between the shattering-susceptible and shattering-resistant vetch accessions, of which 575 were up-regulated and 710 were down-regulated (Figure 8A). Further analysis of the DEGs revealed that 1,087 (84.6%) genes overlapped in different types of pod shattering and that 48 (3.7%) were expressed in only shattering-resistant accessions, and 150 (11.7%) were expressed in only shattering-susceptible accessions (Figure 8B). To obtain an overview of the dependency of the changes in DEG expression, a K-means clustering analysis using MIV was performed to identify the expression patterns of differential genes associated with pod shattering in the two



pod shattering types of common vetch. A total of 1,285 DEGs were clustered into nine distinct clusters with similar expression patterns, including five down-regulated (profile 3, 4, 5, 6, and 7) patterns and four up-regulated (profile 1, 2, 8, and 9) patterns (Figure 9).

GO Functional Analysis of the DEGs

A total of 448 (34.86%) DEGs associated with pod shattering were divided into 51 GO categories (Figure S8). In the cellular component category, “cell part” (26.1%) was the dominant group and was followed by “membrane” (13.2%), and “organelle” (12.3%). For the molecular function category, “catalytic activity” (56.9%) and “binding” (49.1%) were the most dominant groups. Regarding the biological process category, 57.8% and 45.3% of the unigenes were assigned to “metabolic process” and “cellular process.”

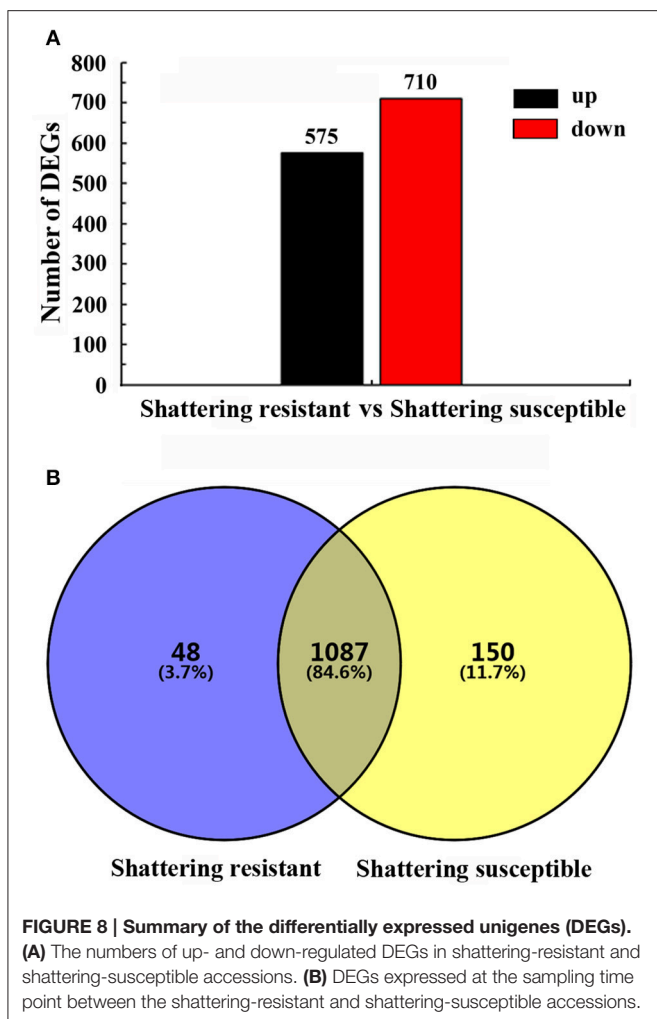
KEGG Pathway Enrichment Analysis of the DEGs

We performed a KEGG pathway enrichment analysis on all 1,285 DEGs to understand the characteristics of the complex biological behavior of the transcriptome. A p -value < 0.05 was considered to indicate significant overexpression of a KEGG pathway. The

enriched and downregulated unigenes in the pod ventral suture of vetch were classified into 50 functional groups. The pathways categorized as “starch and sucrose metabolism” (ko00500) and “pentose and glucuronate interconversions” (ko00040) were found to be significantly overexpressed and the number of up-regulated unigenes was significantly higher than the number of down-regulated unigenes (Figure S9). The “pectin metabolism” was included in the pathways of both ko00040 and ko00500, while the “cellulose metabolism” was only included in the ko00040 pathways. Pectin and cellulose are the main components of the plant cell wall, and its hydrolysis and metabolism have a significant effect on cell wall degradation.

Identification of Pod Shattering-Related Genes

A large number of unigenes were obtained in this study, of which 22 DEGs were considered to be involved in pod shattering (Figure 10). Most of these unigenes encoding cell wall modification enzymes and were significantly highly expressed in the shattering-susceptible accessions. These unigenes included one pectate lyase, one β -galactosidase, one glucuronokinase, two pectinesterase, two glucanases, two polygalacturonases, four



chitinases and eight glucosidases. We used agriGO to analyze the DEGs (FDR < 0.05, FC \geq 1.3) of related pod shattering enriched in the molecular function, cellular component and biological processes terms “enrichment status” and “hierarchy.” In the unigenes that were highly expressed in the shattering-susceptible accessions, nine GO enrichment terms, such as “iron ion binding,” “hydrolase activity,” and “cationic binding” in the molecular functions category, contained known shatter-related genes (Table S5). These shatter-related hydrolases mainly included β -glucosidase, endo- β -1,3-glucosidase and endo- β -1,3;1,4-glucanase (Figure 10). Many shatter-related hydrolases highly expressed in the shattering-susceptible accessions were also predicted to be enriched in the “extracellular region,” “membrane,” and “cytoplasm” in the cellular component terms (Table S5), and were annotated as expansin, chitinase, and glucuronokinase involved in cell wall modification (Figure 10). In the biological process terms, genes involved in “oxidation reduction,” “carbohydrate metabolic process,” and “carbohydrate catabolic process” were significantly enriched and all included shatter-related genes (Table S5). These shatter-related genes were mainly included chitinase, β -galactosidase

and endo-polygalacturonase (Figure 10). Among them, pectinesterase, polygalacturonase, glucuronidase, and one of the glucanases are mainly involved in pectin metabolism, whereas glucosidase and the other glucanase are mainly involved in cellulose metabolism (Figure S10). We also detected expansin and chitinase, which play important roles in cell wall decomposition. Two unigenes encoding cellulase synthase were detected, which were significantly more highly expressed in the shattering-resistant accessions (Figure S11A). Besides these previously identified pod shatter-related genes, other DEGs could also likely be involved in pod shattering in the vetch. The data of DEGs transcripts, all unigenes transcripts and the annotation of 1,285 DEGs (Table S6) have been deposited in the Harvard dataverse (doi: 10.7910/DVN/RJSEP5).

DISCUSSION

Sequence Quality and Annotation

The Illumina platform was initially used only to analyse sequences from species with a reference genome because of its short read length. With improvements in the read length of paired-end sequencing and the development of bioinformatics and computational methods, relatively short reads can also be efficiently assembled for non-model species analysis. In addition, previous studies have shown that compared with other sequencing platforms, the Illumina system provides higher quality and longer sequences, which are well assembled and can be used for transcriptome analysis (Fu et al., 2013; Liu et al., 2016).

In this study, a total of more than 143 million raw reads were produced by using the HiSeq 2000 system, with more than 30 million raw reads from each sample. These raw reads were eventually assembled into 70,742 unigenes with an average length of 772 bp (Figure S3). The average length of the unigenes was also longer than the length of the transcriptome sequences obtained by using the same platform, such as *V. sativa* (503 bp), *V. sativa* subsp. *sativa* (331 bp), *V. sativa* subsp. *nigra* (342 bp) (Kim et al., 2015), *Litchi chinensis* (601 bp) (Li et al., 2013), and *Elymus sibiricus* (645 bp) (Zhou et al., 2016). The results showed that more than 66% of the unigenes matched with functional annotations in public databases, a value higher than previously reported for *V. sativa* (33%) (Sagar et al., 2015), *L. chinensis* (59%) (Li et al., 2013), and *Mangifera indica* (62%) (Dautt-Castro et al., 2015). In addition, the qRT-PCR results demonstrated that our sequencing was accurate and reliable. Unannotated unigenes may represent untranslated regions, non-coding RNA, mis-assembly, or a common vetch-specific gene pool (Fu et al., 2013; Liu et al., 2016). These unigenes, which represent common vetch-specific genes, should serve as a useful complement to the current vetch database.

Twenty-two DEGs were found to be involved in pectin and cellulose metabolism or cell wall modifications. These results should help researchers understand the function of the genes that cause pod shattering in vetch and may serve as a reference for studies of pod shattering in other species, and facilitate further breeding programmes aimed at producing shattering-resistant crops.

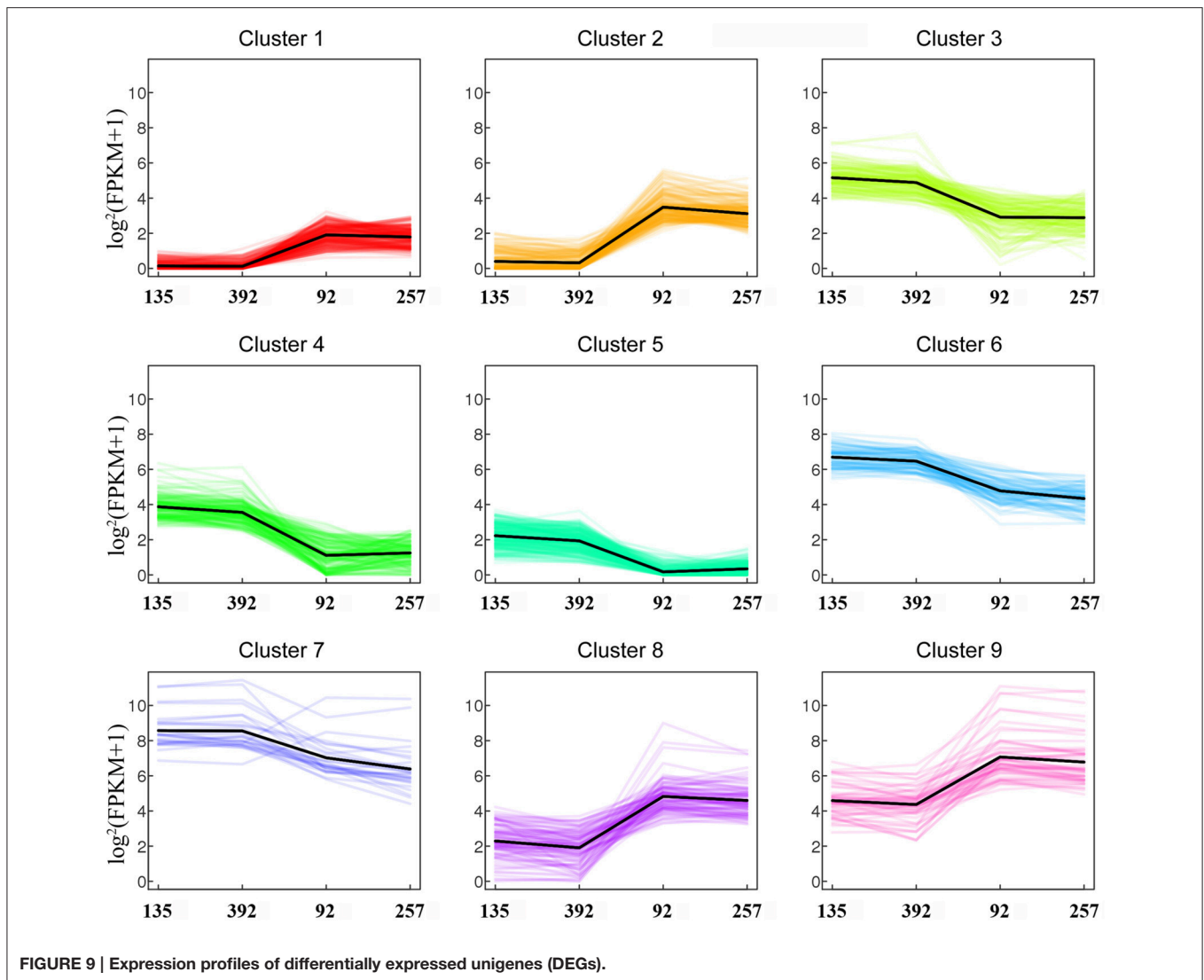
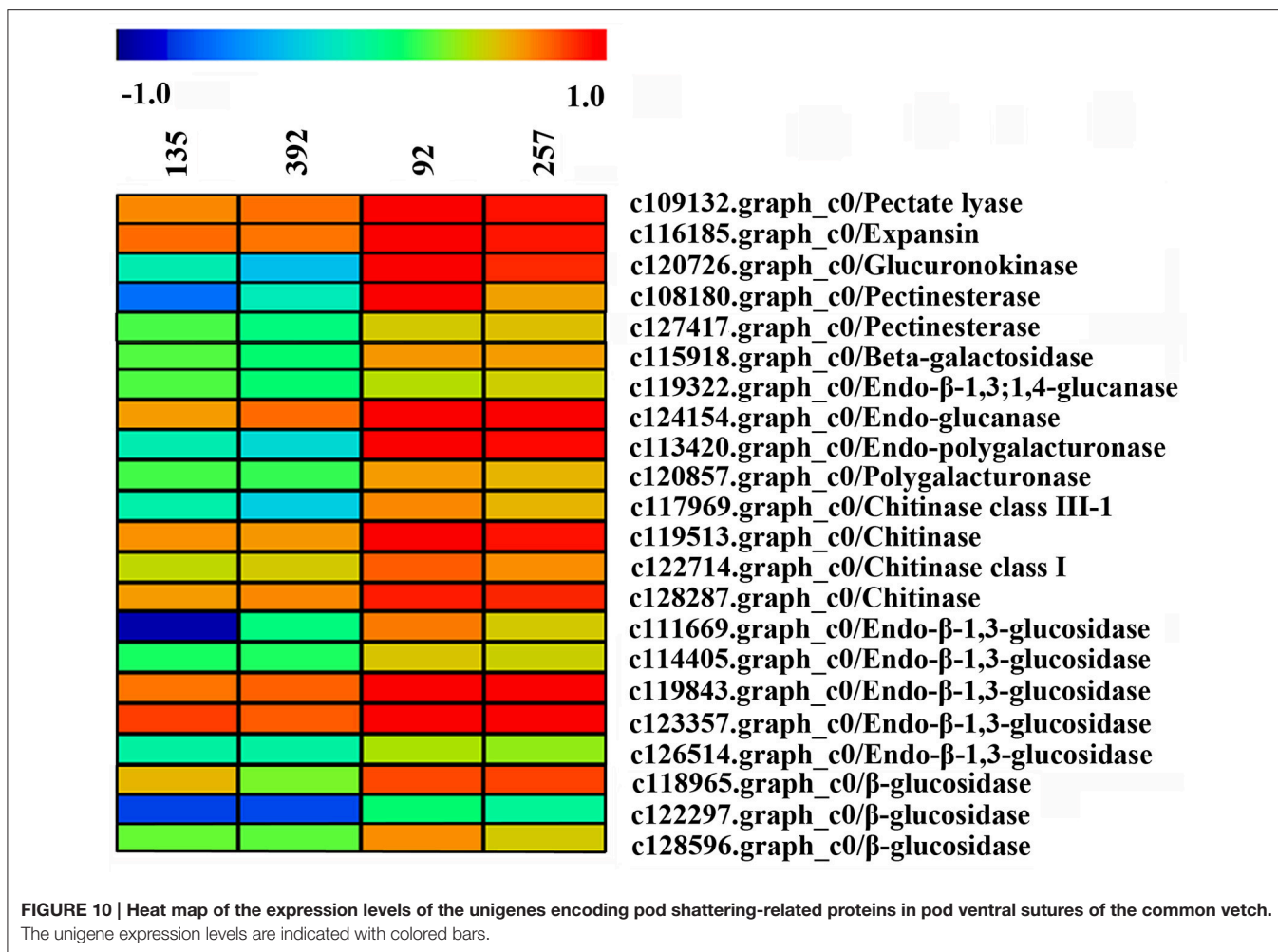


FIGURE 9 | Expression profiles of differentially expressed unigenes (DEGs).

Genes Associated With Pod Shattering

Previous studies have shown that alterations in the cell structure of the dehiscence zone is one of the main causes of pod shattering (Dong et al., 2014). However, the breakdown of the dehiscence zone is dependent on a variety of cell wall modification enzymes and genes that cause cell structure changes, such as endo-polygalacturonase (Christiansen et al., 2002), glucosidase (Muriira et al., 2015), *SHATTERPROOF1* (*SHP1*), *SHATTERPROOF2* (*SHP2*) (Liljegren et al., 2000), *SHAT1-5* (Dong et al., 2014), and *pdh1* (Funatsuki et al., 2014). The use of QTLs mapping has been able to successfully isolate and characterize the plant structure, seed shredding and pod shattering genes in rice (*Oryza sativa*), maize (*Zea mays*) and tomato (*Lycopersicon esculentum*) (Li et al., 2006; Dong et al., 2014). Over the past 15 years, a series of genomic regions associated with soybean pod shattering have been identified by high-resolution mapping of QTLs (Yamada et al., 2009; Dong et al., 2014). *qPDH1* is a QTL for pod shattering that are

fine-mapped in the 134 kb region of chromosome 16 (Suzuki et al., 2010). It was found that *SHAT1-5* associated with soybean pod shattering had hitchhiking effect on closely linked loci across 116 kb region in chromosome 16 of the soybean genome (Dong et al., 2014). Analyses of enzyme activity have also shown that there are significant differences in the pod ventral sutures between shattering-susceptible and shattering-resistant soybean varieties (Agrawal et al., 2002; Christiansen et al., 2002). It has been reported that pectin and cellulose are the main components of the plant cell wall, and their content in the cell wall significantly affects the cell structure (Jung and Park, 2013; Muriira et al., 2015). In the present study, 22 DEGs associated with cell wall modification enzymes were detected, all of which were up-regulated in the shattering-susceptible accessions. In particular, the unigenes encoding several significantly over-represented enzymes involved in the metabolism of pectin and cellulose were identified in the “starch and sucrose” (ko00500) and “pentose and glucuronate interconversion” (ko00040)



metabolism pathways. These unigenes included pectinesterase (EC:3.1.1.11), polygalacturonase (EC:3.2.1.15), glucuronokinase (EC:2.7.1.43), endo-glucanase (EC:3.2.1.4), and glucosidase (EC:3.2.1.21) (Figure S10). The validation of polygalacturonase activity and cellulose (β-1,3;1,4-glucanase) activity was also consistent with the expression levels of unigenes encoding polygalacturonase and cellulose, as determined by transcriptome sequencing (Figures 4, 5, 10).

Pectin and Cellulose Metabolism Is Associated with Pod Shattering

Pectin is the major component of the intercellular layer of plant cell walls. In the pectin metabolism pathway, pectin is de-esterified by pectinesterase (c108180.graph_c0 and c127417.graph_c0) hydrolysis, thus causing pectic chain esterification and production of pectate, which is further hydrolysed by polygalacturonase (c120857.graph_c0) and exo-polygalacturonase to D-galacturonate. D-galacturonate is indirectly hydrolysed to D-glucuronate, whereas D-glucuronate is further hydrolysed by glucuronokinase (c120726.graph_c0) thus, the finally generating UDP-glucose (Zhang et al., 2015) (Figure S10A). With the accumulation

of endo-polygalacturonase (c113420.graph_c0) activity, the middle lamella gradually dissolves and disappears, and the modification of the cell wall becomes evident (Christiansen et al., 2002). In addition to the dissolution of the middle lamella, endo-polygalacturonase also act synergistically with glucanase (c119322.graph_c0 and c119843.graph_c0), thus weakening the primary walls of the cells in the dehiscence zone (Christiansen et al., 2002). Pectate lyase (c109132.graph_c0) is thought to involve demethylation of the pectin and thus to promote the breakdown of the cell wall middle lamella (Patterson, 2001). According to previous studies, endo-polygalacturonase breaks down the pectin network in the cell wall, whereas glucanase destroys the xyloglucan network, thereby significantly destabilizing the cell wall and, in the final phase of programmed cell death, allowing cells and protoplasts to collapse (Groover and Jones, 1999; Christiansen et al., 2002). Internal turgor pressure loss due to tonoplast rupture may cause cell and primary cell wall deformation (Christiansen et al., 2002), thereby significantly widening the gap in the dehiscence zone and causing the pod to shatter more easily.

Cellulose, a cell wall polysaccharide, is a major component of the plant cell wall structure and serves as a scaffold for

binding to other plant cell wall components (Lerouxel et al., 2006; Muriira et al., 2015). Previous studies have shown that an extensive hydrogen-bonding network formed between the cellulose microfibril and the hemicellulose xyloglucan is an important load-bearing structure in the primary wall in dicots (Rose and Bennett, 1999). In cellulose metabolism, cellulose is first hydrolysed by endo-glucanase (c124154.graph_c0) and exo-cellobiohydrolase, thus producing cellobiose and 1,4- β -D-glucan. Cellobiose and 1,4- β -D-glucan are further hydrolysed by β -glucosidase (c118965.graph_c0; c122297.graph_c0; c128596.graph_c0), thereby producing β -D-glucose (Figure S10B). Interestingly, two unigenes (c115986.graph_c0 and c122597.graph_c0) involved in cellulose synthesis were detected, and their expression levels were significantly higher in shattering-resistant accessions than in shattering-susceptible accessions (Figure S11A). This result showed that the rate of cellulose synthesis was low and the cellulose metabolic rate was high in pod ventral sutures of shattering-susceptible accessions, thus further aggravating the breakdown of dehiscence zone cells. Moreover, expansin (c116185.graph_c0), a synergistic enzyme in plant cell walls, is also important for coordinated wall disassembly in plant cells (Rose and Bennett, 1999). It is possible to mediate cell wall loosening or swelling by modifying the cellulose and xyloglucan network, thereby altering the substrate availability for the hydrolase and/or transglycosylase of the host (Rose and Bennett, 1999).

Other Enzymes and Functional Genes Associated with Pod Shattering

Abscission involves cell wall dissolution or cell separation, which is thought to be related to cell wall destruction through the action of chitinases (Xie et al., 2011). In *Calotropis procera*, the expression of chitinase increases with fruit dehiscence (Ibrahim et al., 2016). Furthermore, a promoter-GUS construct of the chitinase gene is strongly expressed in the floral organs of *Arabidopsis* (Patterson, 2001). In the present study, four unigenes (c117969.graph_c0; c119513.graph_c0; c122714.graph_c0; c128287.graph_c0) encoding chitinase were strongly expressed in the shattering-susceptible accessions, thus suggesting that they are also involved in the cell wall dissolution or cell separation of the pod ventral suture zone.

Other hydrolases are also involved in the decomposition of the cell wall polysaccharide matrix and network, such as β -galactosidase (c115918.graph_c0). β -Galactosidase also plays an important role in the softening of apples and Japanese pears (Li et al., 2015).

Previous studies have shown that *Lepidium appelianum* fruits cannot be opened. The anatomical structure of *L. appelianum* fruits indicates a lack a dehiscence zone, and the fruits are surrounded by a continuous loop of lignified cells (Mühlhausen et al., 2013). Mühlhausen et al. (2013) have found that *APETALA2* (*AP2*) is a negative regulator of *SHPI1*, *SHPI2*, and *RPL*, and it inhibits the overexpression of these genes in the replum and valve margin of the *L. appelianum* fruit, thereby preventing fruit shattering. However, in our study, there were

no significant differences in the expression level of the unigene (c125518.graph_c0) with a sequence homologous to that of the *AP2* gene detected in the two types of accessions. Other genes associated with soybean and *Arabidopsis* pod shattering, such as *SHAT1-5*, *pdh1*, *SHPI1*, *SHPI2*, *IND*, and *ALC*, were also not detected as differentially expressed unigenes and were low homology with our sequencing data (Figure S11B). *SHAT1-5* (Glyma16g02200) is specifically expressed in the FCC of the soybean, while *pdh1* (Glyma16g25600) is specifically expressed in the lignin-rich inner sclerenchyma of soybean pod walls. However, their putative homologs in vetch did not differently expressed between shattering-susceptible and shattering-resistant accessions. It can be explained by the different sample tissues and different anatomy between the species. There is no FCC in the pod ventral sutures of the vetch (unpublished data, submitted to Crop Science), and the present study did not include the inner sclerenchyma tissue (Figure 6). Fruit structures are highly labile during evolution, and molecular phylogenetic data consistently show that many species with similar fruit may be only distantly related, whereas species with significantly different fruit may be very closely related (Mühlhausen et al., 2013). In addition, the sampling period of pods in this study was not consistent with that in other studies, because the developmental stages of pods are not the same among different species. Thus, our results may indicate that other genes in the common vetch may have the same function as *AP2* or other pod shattering-related genes or that there was no significant difference in the unigene expression levels, owing to inconsistencies in the sampling time. This result may aid in further study the function of genes related to common vetch pod shattering.

CONCLUSION

In this study, a unigene analysis was performed using clustering, Gene Ontology and KEGG metabolic enrichment pathways analyses, and 1,285 differentially expressed genes were identified between two shattering-susceptible accessions and two resistant accessions. A set of significantly over-represented unigenes involved in the metabolism of pectin and cellulose in the pod ventral sutures of the shattering-susceptible common vetch accessions were identified in the “starch and sucrose” and “pentose and glucuronate interconversions” metabolism pathways. In addition, we proved that a variety of cell wall hydrolases were involved in the cellular metabolism of the pod ventral suture, which promoted pod shattering. A detailed investigation of the candidate genes associated with pod shattering identified in this study would not only deepen understanding of the common vetch pod shattering mechanism but also contribute to the study of pod shattering in other plants and provide information for the molecular breeding of crops.

AUTHOR CONTRIBUTIONS

ZL conceived the topic. RD, DD, DL, QZ, and XC performed the experiments. RD, JZ, WX, YD, and WL analyzed all data. RD wrote the manuscript. ZL and YW revised the manuscript.

ACKNOWLEDGMENTS

This research was supported by the National Basic Research Program of China (2014CB138704), the National Natural Science Foundation of China (31672476). The authors express their sincere thanks to the US National Plant Germplasm System (NPGS) for providing the accessions used in the study. We also acknowledge Yinzheng Wang in Institute of Botany, the Chinese Academy of Sciences, and Kai Luo, Zhengshe Zhang, Rui Zhang, and Xueyang Min in Lanzhou University for their valuable help and advice.

SUPPLEMENTARY MATERIAL

The Supplementary Material for this article can be found online at: <http://journal.frontiersin.org/article/10.3389/fpls.2017.00649/full#supplementary-material>

Figure S1 | Clean reads in the sample libraries from the four common vetch accessions.

Figure S2 | The distribution of the contig assembly.

Figure S3 | Length distribution of the assembled unigenes.

Figure S4 | A species-based distribution of BLASTX matches in the NCBI non-redundant (Nr) database.

Figure S5 | Gene Ontology (GO) classification of the assembled transcripts.

Figure S6 | Clusters of orthologous groups (COGs) function classifications of the assembled transcripts.

Figure S7 | Pathway assignment based on Kyoto Encyclopedia of Genes and Genomes (KEGG). (A) Classification based on metabolism categories. **(B)** Eighteen metabolism subcategories classified by KEGG.

Figure S8 | Gene Ontology (GO) classification of the DEGs. The unigenes were summarized in three main categories: biological process, cellular location, and molecular function.

Figure S9 | Metabolism pathway assignments of the differentially expressed unigenes (DEGs) based on the Kyoto Encyclopedia of Genes and Genomes (KEGG). The genes were classified into 50 functional groups. Positive and negative numbers denoted the percentages of unigenes enriched and downregulated.

REFERENCES

- Abd El-Moneim, A. M. (1993). Selection for non-shattering common vetch, *Vicia sativa* L. *Plant Breed.* 110, 168–171. doi: 10.1111/j.1439-0523.1993.tb01231.x
- Agrawal, A. P., Basarkar, P. W., Salimath, P. M., and Patil, S. A. (2002). Role of cell wall-degrading enzymes in pod-shattering process of soybean, *Glycine max* (L.) Merrill. *Curr. Sci. India* 82, 58–60.
- Anders, S., and Huber, W. (2010). Differential expression analysis for sequence count data. *Genome Biol.* 11:1. doi: 10.1186/gb-2010-11-10-r106
- Benjamini, Y., and Hochberg, Y. (1995). Controlling the false discovery rate: a practical and powerful approach to multiple testing. *J. R. Stat. Soc. B.* 57, 289–300.
- Bhor, T. J., Chimote, V. P., and Deshmukh, M. P. (2014). Inheritance of pod shattering in soybean [*Glycine max* (L.) Merrill]. *Electr. J. Plant Breed.* 5, 671–676.
- Calzadilla, P. I., Maiale, S. J., Ruiz, O. A., and Escaray, F. J. (2016). Transcriptome response mediated by cold stress in *Lotus japonicus*. *Front. Plant Sci.* 7:374. doi: 10.3389/fpls.2016.00374

Figure S10 | Simplified diagram depicting the pectin and cellulose metabolism pathways in pod ventral sutures of the common vetch. (A) Pectin metabolism pathway. **(B)** Cellulose metabolism pathway. The red box indicates that the gene encoding the enzyme is a DEG. The coloured boxes represent the expression levels of the genes encoding the same enzyme in the four accessions.

Figure S11 | Heat map of the expression levels of unigenes encoding other pod shattering-related proteins in pod ventral sutures of the common vetch. (A) Heat map of unigenes encoding cellulose synthase. **(B)** Heat map of unigenes encoding *AP2*, *SHAT1-5*, *pdh1*, *IND*, and *ALC*. Unigene expression levels are indicated with colored bars.

Table S1 | The sampling time of different accessions, the size of the mature seeds and pods, and the number of days required for the pods to reach the mature yellow stage. The sampling time is the number of days from the day of flowering to the day of sampling. Mature seed length and width refer to the length and width of the seed when the pod reached the mature yellow stage. Mature pod length and width refer to the length and width of the pod when the pod reached the mature yellow stage. Mature yellow pod refers to the number of days required for the pods to reach the mature yellow stage.

Table S2 | Primers used for qRT-PCR analysis. Unigene 68614 was used as an internal control in the qRT-PCR analysis.

Table S3 | BLAST analysis of the non-redundant unigenes against public databases.

Table S4 | KEGG pathway analysis of the assembled unigenes.

Table S5 | Gene Ontology (GO) biological process, cellular component, and molecular function term “enrichment status” of the pod ventral suture-specific differentially expressed unigenes (DEGs). The DEGs exhibited an FC \geq 1.3. The FDR-adjusted *p*-values < 0.05. The P refers to the biological process. The F refers to molecular function. The C refers to cellular component. The “*” indicates the GO term containing the unigenes associated with the pod shattering.

Table S6 | A list of 1,285 differentially expressed unigenes (DEGs) in pod ventral sutures of shattering-susceptible and shattering-resistant vetch accessions. No. 135 and No. 392 are shattering-susceptible accessions. No. 92 and No. 257 are shattering-resistant accessions. FPKM refers to the Fragments Per Kilobase per Million Fragments mapped. The C refers to the Gene Ontology. COG refers to the Clusters of Orthologous Groups of proteins. KEGG refers to the Kyoto Encyclopedia of Genes and Genomes. KOG refers to the eukaryotic Ortholog Groups. Swissprot refers to the Swiss-Prot protein databases. Pfam refers to the Pfam protein database. nr refers to the NCBI non-redundant protein sequences. “–” Indicates that the unigene was not successfully annotated in the corresponding database.

- Christiansen, L. C., Dal Degan, F., Ulvskov, P., and Borkhardt, B. (2002). Examination of the dehiscence zone in soybean pods and isolation of a dehiscence-related endopolygalacturonase gene. *Plant Cell Environ.* 25, 479–490. doi: 10.1046/j.1365-3040.2002.00839.x
- Chung, J. W., Kim, T. S., Suresh, S., Lee, S. Y., and Cho, G. T. (2013). Development of 65 novel polymorphic cDNA-SSR markers in common vetch (*Vicia sativa* subsp. *sativa*) using next generation sequencing. *Molecules* 18, 8376–8392. doi: 10.3390/molecules18078376
- Dautt-Castro, M., Ochoa-Leyva, A., Contreras-Vergara, C. A., Pacheco-Sanchez, M. A., Casas-Flores, S., and Sanchez-Flores, A. (2015). Mango (*Mangifera indica* L.) cv. Kent fruit mesocarp de novo transcriptome assembly identifies gene families important for ripening. *Front. Plant Sci.* 6:62. doi: 10.3389/fpls.2015.00062
- del Carmen Rodríguez-Gacio, M., Nicolás, C., and Matilla, A. J. (2004). Cloning and analysis of a cDNA encoding an endo-polygalacturonase expressed during the desiccation period of the silique-valves of turnip-tops (*Brassica rapa* L. cv. Rapa). *J. Plant Physiol.* 161, 219–227. doi: 10.1078/0176-1617-01153
- Dong, R., Dong, D. K., Shao, K. Z., Zhou, Q., Chai, X. T., and Dong, Y. (2016b). The digital evaluation of the cracking force of common vetch with

- the different characteristics of pod shattering. *Pratacult. Sci.* 33, 2511–2517. doi: 10.11829/j.issn.1001-0629.2015-0704
- Dong, R., Jahufer, M. Z. Z., Dong, D. K., Wang, Y. R., and Liu, Z. P. (2016a). Characterisation of the morphological variation for seed traits among 537 germplasm accessions of common vetch (*Vicia sativa* L.) using digital image analysis. *New Zeal. J. Agr. Res.* 59, 422–435. doi: 10.1080/00288233.2016.1229682
- Dong, Y., Yang, X., Liu, J., Wang, B. H., Liu, B. L., and Wang, Y. Z. (2014). Pod shattering resistance associated with domestication is mediated by a NAC gene in soybean. *Nat. Commun.* 5:3352. doi: 10.1038/ncomms4352
- Firincioglu, H. K. (2012). A comparison of six vetches (*Vicia* spp.) for developmental rate, herbage yield and seed yield in semi-arid central Turkey. *Grass Forage Sci.* 69, 303–314. doi: 10.1111/gfs.12021
- Fu, N., Wang, Q., and Shen, H. L. (2013). *De novo* assembly, gene annotation and marker development using Illumina paired-end transcriptome sequences in celery (*Apium graveolens* L.). *PLoS ONE* 8:e57686. doi: 10.1371/journal.pone.0057686
- Funatsuki, H., Ishimoto, M., Tsuji, H., Kawaguchi, K., Hajika, M., and Fujino, K. (2006). Simple sequence repeat markers linked to a major QTL controlling pod shattering in soybean. *Plant Breeding* 125, 195–197. doi: 10.1111/j.1439-0523.2006.01199.x
- Funatsuki, H., Suzuki, M., Hirose, A., Inaba, H., Yamada, T., and Hajika, M. (2014). Molecular basis of a shattering resistance boosting global dissemination of soybean. *Proc. Natl. Acad. Sci. U.S.A.* 111, 17797–17802. doi: 10.1073/pnas.1417282111
- Grabherr, M. G., Haas, B. J., Yassour, M., Levin, J. Z., Thompson, D.A., and Amit, I. (2011). Fulllength transcriptome assembly from RNA-Seq data without a reference genome. *Nat. Biotechnol.* 29, 644–652. doi: 10.1038/nbt.1883
- Groover, A., and Jones, A. M. (1999). Tracheary element differentiation uses a novel mechanism coordinating programmed cell death and secondary cell wall synthesis. *Plant Physiol.* 119, 375–384. doi: 10.1104/pp.119.2.375
- Gross, K. C. (1982). A rapid and sensitive spectrophotometric method for assaying polygalacturonase using 2-cyanoacetamide. *HortScience* 17, 933–934.
- Hadfield, K. A., and Bennett, A. B. (1998). Polygalacturonases: many genes in search of a function. *Plant Physiol.* 117, 337–343. doi: 10.1104/pp.117.2.337
- Hong, S. B., and Tucker, M. L. (1998). Genomic organization of six tomato polygalacturonases and 5' upstream sequence identity with *tap1* and *win2* genes. *Mol. Gen. Genet.* 258, 479–487. doi: 10.1007/s004380050758
- Ibrahim, A. H., Al-Zahrani, A. A., and Wahba, H. H. (2016). The effect of natural and artificial fruit dehiscence on floss properties, seed germination and protein expression in *Calotropis procera*. *Acta. Physiol. Plant.* 38, 1–11. doi: 10.1007/s11738-015-2033-2
- Jarvis, M. C., Briggs, S. P. H., and Knox, J. P. (2003). Intercellular adhesion and cell separation in plants. *Plant Cell Environ.* 26, 977–989. doi: 10.1046/j.1365-3040.2003.01034.x
- Jung, J., and Park, W. (2013). Comparative genomic and transcriptomic analyses reveal habitat differentiation and different transcriptional responses during pectin metabolism in *Alishewanella* species. *Appl. Environ. Microb.* 79, 6351–6361. doi: 10.1128/AEM.02350-13
- Kawamoto, T. (2003). Use of a new adhesive film for the preparation of multi-purpose fresh-frozen sections from hard tissues, whole-animals, insects and plants. *Arch. Histol. Cytol.* 66, 123–143. doi: 10.1679/aohc.66.123
- Kim, T. S., Raveendar, S., Suresh, S., Lee, G. A., Lee, J. R., and Cho, J. H. (2015). Transcriptome analysis of two *Vicia sativa* subspecies: mining molecular markers to enhance genomic resources for vetch improvement. *Genes* 6, 1164–1182. doi: 10.3390/genes6041164
- Langmead, B., and Salzberg, S. L. (2012). Fast gapped-read alignment with Bowtie 2. *Nat. Methods* 9, 357–359. doi: 10.1038/nmeth.1923
- Langmead, B., Trapnell, C., Pop, M., and Salzberg, S. L. (2009). Ultrafast and memory-efficient alignment of short DNA sequences to the human genome. *Genome Biol.* 10:1. doi: 10.1186/gb-2009-10-3-r25
- Lashbrook, C. C., and Cai, S. (2008). Cell wall remodeling in Arabidopsis stamen abscission zones: temporal aspects of control inferred from transcriptional profiling. *Plant Signal. Behav.* 3, 733–736. doi: 10.4161/psb.3.9.6489
- Lerouxel, O., Cavalier, D. M., Liepman, A. H., and Keegstra, K. (2006). Biosynthesis of plant cell wall polysaccharides—a complex process. *Curr. Opin. Plant Biol.* 9, 621–630. doi: 10.1016/j.pbi.2006.09.009
- Li, B., and Dewey, C. N. (2011). RSEM: accurate transcript quantification from RNA-Seq data with or without a reference genome. *BMC Bioinformatics* 12:323. doi: 10.1186/1471-2105-12-323
- Li, C. Q., Wang, Y., Huang, X. M., Li, J., Wang, H. C., and Li, J. G. (2013). *De novo* assembly and characterization of fruit transcriptome in *Litchi chinensis* Sonn and analysis of differentially regulated genes in fruit in response to shading. *BMC Genomics* 14:552. doi: 10.1186/1471-2164-14-552
- Li, C., Zhou, A., and Sang, T. (2006). Rice domestication by reducing shattering. *Science* 311, 1936–1939. doi: 10.1126/science.1123604
- Li, X. W., Jiang, J., Zhang, L. P., Yu, Y., Ye, Z. W., and Wang, X. M. (2015). Identification of volatile and softening-related genes using digital gene expression profiles in melting peach. *Tree Genet. Genomes* 11, 1–15. doi: 10.1007/s11295-015-0891-9
- Liljegren, S. J., Ditta, G. S., Eshed, Y., Savidge, B., Bowman, J. L., and Yanofsky, M. F. (2000). SHATTERPROOF MADS-box genes control seed dispersal in *Arabidopsis*. *Nature* 404, 766–770. doi: 10.1038/35008089
- Liu, W. X., Zhang, Z. S., Chen, S. Y., Ma, L. C., Wang, H. C., and Dong, R. (2016). Global transcriptome profiling analysis reveals insight into saliva-responsive genes in alfalfa. *Plant Cell Rep.* 35, 561–571. doi: 10.1007/s00299-015-1903-9
- Liu, Z. P., Chen, T. L., Ma, L. C., Zhao, Z. G., Zhao, P. X., and Nan, Z. B. (2013b). Global transcriptome sequencing using the Illumina platform and the development of EST-SSR markers in autotetraploid alfalfa. *PLoS ONE* 8:e83549. doi: 10.1371/journal.pone.0083549
- Liu, Z. P., Liu, P., Luo, D., Liu, W. X., and Wang, Y. R. (2014). Exploiting Illumina sequencing for the development of 95 novel polymorphic EST-SSR markers in common vetch (*Vicia sativa* subsp. *sativa*). *Molecules* 19, 5777–5789. doi: 10.3390/molecules19055777
- Liu, Z. P., Ma, L. C., Nan, Z. B., and Wang, Y. R. (2013a). Comparative transcriptional profiling provides insights into the evolution and development of the zygomorphic flower of *Vicia sativa* (Papilionoideae). *PLoS ONE* 8:e57338. doi: 10.1371/journal.pone.0057338
- Østergaard, L., Kempin, S. A., Bies, D., Klee, H. J., and Yanofsky, M. F. (2006). Pod shatter-resistant *Brassica*, fruit produced by ectopic expression of the *FRUITFULL* gene. *Plant Biotechnol. J.* 4, 45–51. doi: 10.1111/j.1467-7652.2005.00156.x
- Lohani, S., Trivedi, P. K., and Nath, P. (2004). Changes in activities of cell wall hydrolases during ethylene-induced ripening in banana: effect of 1-MCP, ABA and IAA. *Postharvest Biol. Tec.* 31, 119–126. doi: 10.1016/j.postharvbio.2003.08.001
- Mühlhausen, A., Lenser, T., Mummenhoff, K., and Theissen, G. (2013). Evidence that an evolutionary transition from dehiscent to indehiscent fruits in *Lepidium* (Brassicaceae) was caused by a change in the control of valve margin identity genes. *Plant J.* 73, 824–835. doi: 10.1111/tpj.12079
- Muriira, N. G., Xu, W., Muchugi, A., Xu, J., and Liu, A. (2015). *De novo* sequencing and assembly analysis of transcriptome in the Sodom apple (*Calotropis gigantea*). *BMC Genomics* 16:723. doi: 10.1186/s12864-015-1908-3
- Patterson, S. E. (2001). Cutting loose. Abscission and dehiscence in Arabidopsis. *Plant Physiol.* 126, 494–500. doi: 10.1104/pp.126.2.494
- Pekrun, C., Lutman, P. J., and Baeumer, K. (1997). Induction of secondary dormancy in rape seeds (*Brassica napus* L.) by prolonged imbibition under conditions of water stress or oxygen deficiency in darkness. *Eur. J. Agron.* 6, 245–255. doi: 10.1016/S1161-0301(96)02051-5
- Raman, H., Raman, R., Kilian, A., Detering, F., Carling, J., and Coombes, N. (2014). Genome-wide delineation of natural variation for pod shatter resistance in *Brassica napus*. *PLoS ONE* 9:e101673. doi: 10.1371/journal.pone.0101673
- Rose, J. K., and Bennett, A. B. (1999). Cooperative disassembly of the cellulose-xylolucan network of plant cell walls: parallels between cell expansion and fruit ripening. *Trends Plant Sci.* 4, 176–183. doi: 10.1016/S1360-1385(99)01405-3
- Sagar, S. P., Dipti, B. S., and Panchal, H. J. (2015). *De Novo* RNA seq assembly and annotation of *Vicia sativa* L. (SRR403901). *Genom. Appl. Biol.* 6, 1–7. doi: 10.5376/gab.2015.06.0002
- Shannon, P., Markiel, A., Ozier, O., Baliga, N. S., Wang, J. T., and Ramage, D. (2003). Cytoscape: a software environment for integrated models of biomolecular interaction networks. *Genome Res.* 13, 2498–2504. doi: 10.1101/gr.1239303
- Sivankalyani, V., Sela, N., Feygenberg, O., Zemach, H., Maurer, D., and Alkan, N. (2016). Transcriptome dynamics in mango fruit peel reveals mechanisms of chilling stress. *Front. Plant Sci.* 7:1579. doi: 10.3389/fpls.2016.01579

- Squires, T. M., Gruwel, M. L., Zhou, R., Sokhansanj, S., Abrams, S. R., and Cutler, A. J. (2003). Dehydration and dehiscence in siliques of *Brassica napus* and *Brassica rapa*. *Can. J. Bot.* 81, 248–254. doi: 10.1139/b03-019
- Sullivan, P. G., and Diver, S. (2003). *Overview of Cover Crops and Green Manures*. Fayetteville: NCAT Agriculture Specialist, United States.
- Suzuki, M., Fujino, K., Nakamoto, Y., Ishimoto, M., and Funatsuki, H. (2010). Fine mapping and development of DNA markers for the *qPDH1* locus associated with pod dehiscence in soybean. *Mol. Breeding* 25, 407–418. doi: 10.1007/s11032-009-9340-5
- Tavarini, S., Degl'Innocenti, E., Remorini, D., Massai, R., and Guidi, L. (2009). Polygalacturonase and β -galactosidase activities in hayward kiwifruit as affected by light exposure, maturity stage and storage time. *Sci. Hortic.* 120, 342–347. doi: 10.1016/j.scienta.2008.11.013
- van de Wouw, M., Maxted, N., and Ford-Lloyd, B. V. (2003). Agro-morphological characterisation of common vetch and its close relatives. *Euphytica* 130, 281–292. doi: 10.1023/A:1022899410696
- Wang, L. K., Feng, Z. X., Wang, X., Wang, X. W., and Zhang, X. G. (2010). DEGseq: an R package for identifying differentially expressed genes from RNA-seq data. *Bioinformatics* 26, 136–138. doi: 10.1093/bioinformatics/btp612
- Wu, Y., Deng, Y., and Li, Y. F. (2008). Changes in enzyme activities in abscission zone and berry drop of 'Kyoho' grapes under high O₂ or CO₂ atmospheric storage. *LWT Food Sci. Technol.* 41, 175–179. doi: 10.1016/j.lwt.2007.01.015
- Xie, D., Liang, W., Xiao, X., Liu, X., Chen, L., and Chen, W. (2011). Molecular cloning and characterization of a chitinase gene up-regulated in longan buds during flowering reversion. *Afr. J. Biotechnol.* 10, 12504–12511. doi: 10.5897/AJB10.2669
- Yamada, T., Funatsuki, H., Hagihara, S., Fujita, S., Tanaka, Y., and Tsuji, H. (2009). A major QTL, *qPDH1*, is commonly involved in shattering resistance of soybean cultivars. *Breeding Sci.* 59, 435–440. doi: 10.1270/jsbbs.59.435
- Ye, J., Fang, L., Zheng, H. K., Zhang, Y., Chen, J., and Zhang, Z. J. (2006). WEGO: a web tool for plotting GO annotations. *Nucleic Acids Res.* 34, 293–297. doi: 10.1093/nar/gkl031
- Zhang, A. H., Qiu, L., Huang, L., Yu, X. L., Lu, G., and Cao, J. S. (2012). Isolation and characterization of an anther-specific polygalacturonase gene, *BcMF16*, in *Brassica campestris* ssp. *chinensis*. *Plant Mol. Biol. Rep.* 30, 330–338. doi: 10.1007/s11105-011-0341-2
- Zhang, J., Henriksson, G., and Johansson, G. (2000). Polygalacturonase is the key component in enzymatic retting of flax. *J. Biotechnol.* 81, 85–89. doi: 10.1016/S0168-1656(00)00286-8
- Zhang, Y., Shen, Y. Y., Wu, X. M., and Wang, J. B. (2016). The basis of pod dehiscence: anatomical traits of the dehiscence zone and expression of eight pod shatter-related genes in four species of *Brassicaceae*. *Biol. Plant.* 60, 343–354. doi: 10.1007/s10535-016-0599-1
- Zhang, Z. Y., Jiang, S. H., Wang, N., Li, M., Ji, X. H., and Sun, S. S. (2015). Identification of differentially expressed genes associated with apple fruit ripening and softening by suppression subtractive hybridization. *PLoS ONE* 10:e0146061. doi: 10.1371/journal.pone.0146061
- Zhou, Q., Luo, D., Ma, L. C., Xie, W. G., Wang, Y., and Wang, Y. R. (2016). Development and cross-species transferability of EST-SSR markers in Siberian wildrye (*Elymus sibiricus* L.) using Illumina sequencing. *Sci. Rep.* 6:20549. doi: 10.1038/srep20549

Conflict of Interest Statement: The authors declare that the research was conducted in the absence of any commercial or financial relationships that could be construed as a potential conflict of interest.

Copyright © 2017 Dong, Dong, Luo, Zhou, Chai, Zhang, Xie, Liu, Dong, Wang and Liu. This is an open-access article distributed under the terms of the Creative Commons Attribution License (CC BY). The use, distribution or reproduction in other forums is permitted, provided the original author(s) or licensor are credited and that the original publication in this journal is cited, in accordance with accepted academic practice. No use, distribution or reproduction is permitted which does not comply with these terms.